NUMERICAL INVESTIGATION OF HEAT TRANSFER IN FILM LAYER UNDER SUPERSONIC CONDITION OF CONVERGENT-DIVERGENT TRANSITION

by

Bo ZHANG*, Quan HONG, Yun BAI, Jiquan LI, and Honghu JI

Jiangsu Province Key Laboratory of Aerospace Power System, College of Energy and Power, Nanjing University of Aeronautics and Astronautics, Nanjing, China

Original scientific paper
https://doi.org/10.2298/TSCI190401310Z

The distribution of film cooling effectiveness in supersonic mainstream of circle-rectangular Convergent-Divergent transition has been numerically investigated under different pressure ratios. The shock wave exerted superior influence on film cooling. In supersonic main flow, extra compression waves formed in upstream of the film holes, resulted by the obstruction of the multiple cooling jets. This exerted extra pressure to the boundary-layer, induced adverse pressure gradient, and led to weakening of the film flow attachment ability and decreasing of local cooling effectiveness. Bow oblique shock wave occurred in front of holes, the two oblique bow shaped low pressure zones formed on both sides of the hole, and low cooling effectiveness zones appeared accordingly. The inefficient region at the leading edge of the hole destroyed the film developing between holes, decreased the cooling effectiveness accumulation in the rear part. The decrease of hole incline angle caused an increase of cooling effectiveness, which reduced reverse velocity gradient caused by shock wave in the boundary-layer and improved film attachment. The influence of main flow pressure ratio to film cooling was also investigated, and found with increasing of the ratio, the influence will became even significant.

Key words: *supersonic flow, film cooling, shock wave, convergent-divergent nozzle, heat transfer*

Introduction

In recent years, the inlet gas temperature of the nozzle has gradually increased with the increase thrust of aero-engine. It is widely recognized that film cooling is a useful method to extend the hot components life.

Different from the constant pressure environment in the combustion chamber or somewhere else, mainstream flow of the nozzle could reach supersonic state under certain high pressure ratios (PR), and the free stream parameters changed along downstream in the convergent and divergent sections [1, 2].

Many researchers carried out investigations about shocks in nozzle. Adamson [3] experimentally analyzed nozzle jets and presented a useful method for predicting the location of shock inside the transition, while Carlson and Lewis [4] experimentally confirmed the first Mach disc position under supersonic transitions.

* Corresponding author, e-mail: zhangbo_pe@nuaa.edu.cn

In nozzles, shocks always induced complicated interfere with the boundary. Investigations about the interference of shocks with boundary-layer, turbulent separation, and mechanics of separation by flow and reattachment in interaction regions of shock wave boundary-layer were carried out experimentally and numerically [5, 6]

Shimshi *et al.,* [7] revealed the flow structure changes induced by the PR vibrations between the ambient and the jet. When the film cooling was induced in nozzle, a complex wave structure may be induced inside the nozzle, and cooling gas film made the interactions of the shock wave and boundary even complicated [8, 9].The boundary-layer near the wall interacted by the shock separated, and the shock impingement on the film cooling had great impact on cooling effectiveness.

In the past, many investigations had been carried out on film cooling in supersonic situation. Difference showed among supersonic and subsonic situations in film cooling were mainly due to the main flow compressibity development and shock waves in supersonic main flow [10-13].

O'Connor and Haji-Sheikh [14] investigated numerically about the film cooling in supersonic conditions and obtained a high cooling effectiveness, the results showed CFD models were fitted to study film cooling characteristics in supersonic main flow.

Takita and Masuya [15] showed no significant difference caused by the shock wave on the film cooling through a numerically investigation on film cooling with an impinging shock wave

Back *et al.* [16] carried out the investigation through measuring and numerical methods on flows through convergent nozzles in supersonic situation. They presented the wall pressure distribution in various convergent transitions of 2-D flows, and found that quasi-1-D methods are not applicable in such situations. They presented that flow through the transonic region was dependent on local configuration.

Aupoix *et al*. [17] obtained interesting results through experimentally and numerically studies on film cooling in different situations, which showed that film cooling can obtained high efficient in supersonic flow than subsonic one. Olsen [18] carried out experimental investigation to real the changing of film cooling caused by extended shock wave, and found lower PR shock wave could result increase of cooling effectiveness.

Most of published numerical simulations have been performed on simplified geometries or on specific model configurations. The cooling effectiveness was related to various factors in supersonic conditions, including free stream parameters and cooling gas parameters.

Dutton [19] designed convergent-divergent nozzles and made an optimization on parameter configuration, and found the major effect of swirl on the flow field was to cause large increases in axial velocity near the centerline.

Peng *et al.,* [20] carried out the investigations about the influence of the shock wave intensity on the film cooling in supersonic situation, and further obtained the influence of coolant inlet Mach number and shock wave generator width.

Although many investigations of film cooling in supersonic flow were carried out, researchers focused mainly about the cooling effectiveness. However, what influence that the main flow shock wave brought to coolant jet, and how it worked were still unknown.

A circle-rectangular convergent-divergent transition had been designed in this paper, and film cooling holes had been adopted in the divergent section. This paper focused on the interaction between main flow and coolant, and how it affected the film cooling. Further, the paper also paid attention to influence of PR and injection angle.

Problem description and computational model

Problem description

This present paper focused on the cooling characteristics in supersonic main flow.

Figure 1 presented the schematic structures of computational domain, which included a circular to rectangular convergent-divergent nozzle with an expanding angle of 2° and the downstream field. The nozzle inlet was a circular one with diameter of 126 mm, and the throat was a rectangular of height of 15 mm and width of 60 mm, while the divergent and convergent sections were 80 mm and 200 mm long separately, with 2 mm thick steel wall. The main fluid passed through the convergent-divergent nozzle, accelerated to supersonic state and discharges downstream.

The film cooling structure was arranged on the expanding walls, as showed in fig. 1, and the details of the hole arrangement was showed in fig. 2. The cooling region was totally 150 mm long, hole pitch was 10 mm, and hole spacing was set as 8 mm, hole diameter was 1 mm, inclined angle was 20°. The film configuration was set as a long diamond shape that proved to be an efficient configuration.

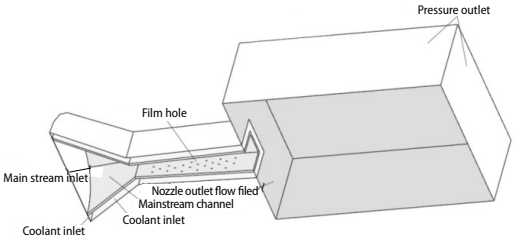

Figure 1. Computational domain and boundary

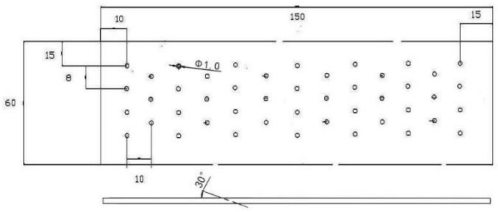

Figure 2. The sketch of film holes configuration

Numerical method

Numerical simulation of this paper was carried out by CFD software fluent and fluid and solid domains are established, respectively, for that the comprehensive cooling effectiveness of film cooling is calculated and analyzed. Flow analysis is carried out by standard k-ε turbulence model and standard wall function of the near-wall area and the flow and heat transfer control equations are discretized by second-order. The convergence is based on the residual of the equation is less than $1 \cdot 10^{-5}$.

The simulations were performed using the CFD software FLUENT, which uses the Favre-averaged equations to analyze the fluid-flow for the continuity, momentum, energy, and mass transport equations. Flow analysis was carried out by standard k-ε turbulence model and standard wall function of the near-wall area, the flow and heat transfer control equations were discretized by second-order. The convergence was based on the residual of the equation is less than $1 \cdot 10^{-5}$.

Considering the symmetry of model, only half model carried out for numerical investigation. Fine structured grid was applied in all fields, and in the region near the wall and the film holes, mesh refinement was adopted to adapt to the rapid change of pressure and velocity gradient, as shown in fig. 3.

To test the validity of the method, a validating case was designed with the same physical model to that of Juhangy *et al.* [13], and carried out under the experimental boundary conditions. Figure 4 presented the comparison of results of this paper and that of [13]. A good agreement of the experimental and numerical results with the Mach number of 1.2 was observed, while at 1.8, the middle of the curve was higher but basically within the acceptable range. The

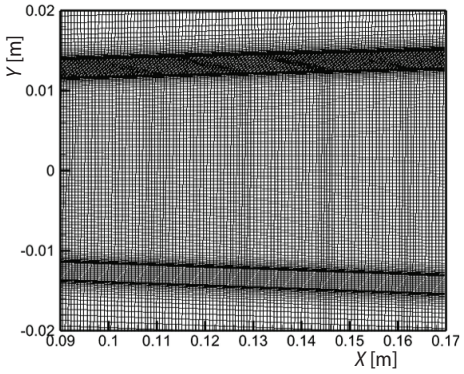

Figure 3. Mesh schematic diagram

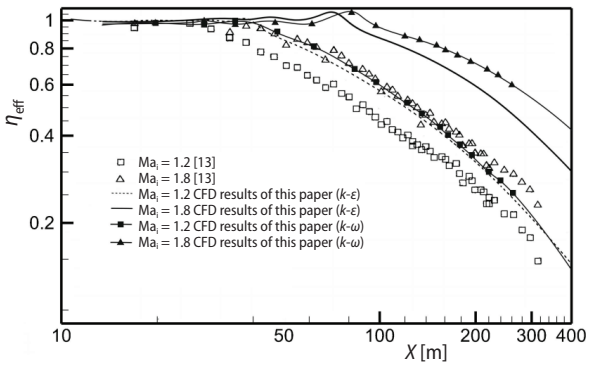

Figure 4. Comparison of results of this paper with [13]

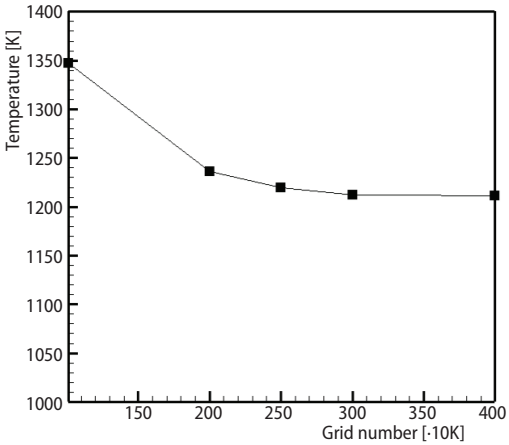

Figure 5. Grid independence test result

comparison results proved the method used in this paper was feasible.

Figure 5 presented the grid independence test result. It can be seen when the number of grids is more than 3 million, the temperature distribution is not affected by the number of grids.

Boundary parameter and solve method

The mainstream total temperature was set as 1200 K, the pressure was determined by the PR (the ratio of the mainstream inlet pressure to the ambient pressure), while ambient temperature was 300 K and pressure was 101 kPa. The cooling stream was supplied by compressor, whose temperature fluctuated in the range of 300~360 K, in the influence of different PR. And the cooling stream pressure was computed from the PR.

Case 1-6 with different PR (1.1-4) in same geometrical parameters were designed to investigate the influence of PR, while Case 6 and Case 7 with different inclined angle (30°, 15°) focused on the effect of inclined angle. All the cases were carried out under same blowing ratio 0.1, tab. 1.

Results and analysis

Distribution of cooling effectiveness

The film cooling effectiveness was defined:

$$\eta = \frac{T_{\mathrm{rg}} - T_{\mathrm{w}}}{T_{\mathrm{rg}} - T_{\mathrm{rc}}} \tag{1}$$

where T_{rg}, T_{rc} are the recovery temperatures of mainstream and coolant stream, separately T_w was the wall surface temperature.

The blowing ratio was defined:

$$M = \frac{\rho_c u_c}{\rho_h u_h} \quad (2)$$

where ρ_h, u_h are density and velocity of the main stream and ρ_c, u_c are density and velocity of the coolant gas.

Figure 6 showed the cooling effectiveness contour maps on the surface of the divergent wall in Case 1-6.

Table 1. The CFD cases

Case	Hole angle [°]	Pressure ratio	Blowing ratio
1	30	1.1	0.1
2	30	1.5	0.1
3	30	2.5	0.1
4	30	3.0	0.1
5	30	3.5	0.1
6	30	4.0	0.1
7	15	4.0	0.1

The film cooling effectiveness distribution under PR 1.1 was shown in fig. 6(a). It could be seen that an increasing of cooling effectiveness occurred in the downstream of the film hole, and then, the cooling effectiveness gradually decreased as the coolant flew downstream, and in the rear of the wall, the gas film formed continuous covering and caused an slightly increasing effectiveness by film accumulation in the rear part, similar with those of subsonic conditions.

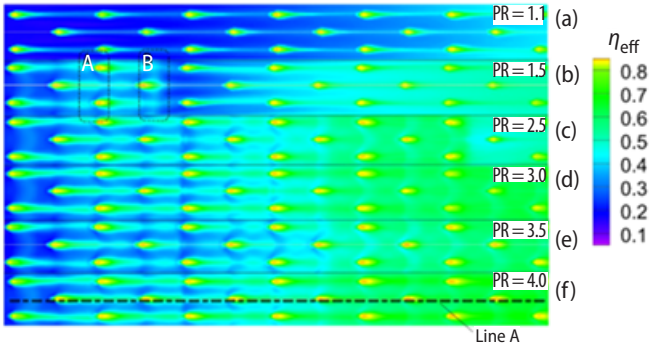

Figure 6. Cooling effectiveness contours of different PR

The cooling effectiveness distribution at PR = 1.5 in fig. 6(b) was similar to fig. 6(a), but the value significantly increased. An effective connection between the adjacent film holes formed in the front part of the wall, and both the lateral and axial spreading of the gas film enhanced, as shown by frame A and B. Cooling effectiveness contour maps remained similar, as PR increased from 1.5 to 2.5 fig. 6(c). Film accumulation between adjacent holes interrupted, caused by the bow shaped low efficient zones, covering several rows of holes. The distribution in PR = 3-4, figs. 6(d)-6(f), remained the similar distribution, while the bow low-efficient zones covered a longer region with the increase of PR.

To be clarity, line A was given passing through the center of the film hole, seen in fig. 6(f). Figure 7 presented the cooling effectiveness on line A under different PR, and the film holes position showed below. When the PR equaled 1.1, the effectiveness increased a little in front of the hole, reached to a peak value on the hole exit region, then decreased in the downstream. It increased again as moved near next hole; the effectiveness showed a growing trend as the coolant gas passed along adja-

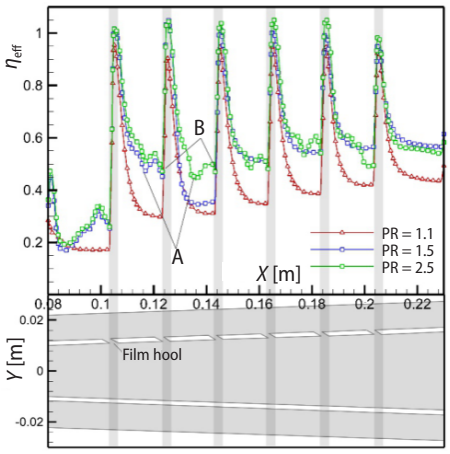

Figure 7. Cooling effectiveness on line A in different PR

cent film holes in axial direction. When the PR grew up to 1.5, the effectiveness downstream the hole increased, but vibration generated which supposed to caused by the influence of interfere of shock wave with boundary-layer [12].

The cooling effectiveness under PR = 2.5 was similar with that of PR = 1.5, while effectiveness value grew higher. The pressure and temperature of main stream decreased in the divergent transition, and the lower pressure led over-expanded of coolant at the hole exit, which brought an decrease of coolant temperature. Both the decrease of temperature and pressure caused the increase of effectiveness. The effectiveness fluctuations between adjacent holes may be caused by pressure variations in boundary-layer.

Correspondence between temperature and pressure

Figure 8 presented the wall pressure and wall temperature distributions along line A under different PR. As aforementioned, the effectiveness vibration may caused by the pressure

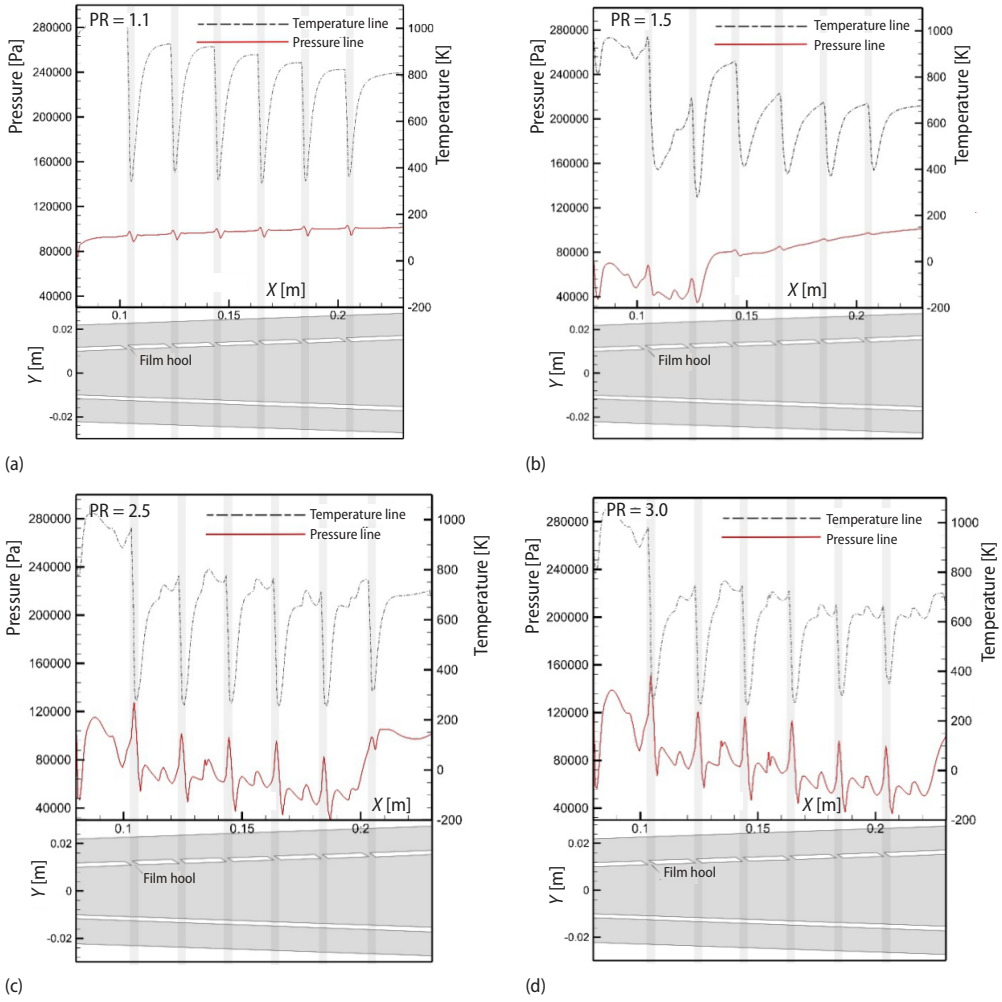

Figure 8. Distribution of temperature and pressure on line A under different PR; (a) PR = 1.1, (b) PR = 1.5, (c) PR = 2.5, and (d) PR = 3.0

fluctuation. Figure 8(a) showed the distribution under PR = 1.1, the pressure and temperature on the wall both showed a strong regularity. Pressure increased slightly along the axial, while little fluctuation occurred on hole exits. However, the temperature always decreased in front of the film holes, and increased again crossing the holes, and totally, the temperature decreased gradually along the axial direction. When PR increased to 1.5, fig. 8(b), the interference between jets and shock wave destroyed the regularity of pressure and temperature. The pressure showed a strongly fluctuation in the front of the wall, and recovered similar regularity with that of PR = 1.1 at downstream, with a decrease of pressure. The temperature also showed a strongly fluctuation in the corresponding region.

As PR increased to 2.5 and 3.0, figs. 8(c) and 8(d), the distribution of pressure and temperature coincided with that of PR = 1.5. High PR increased shock wave intensity, made the fluctuation of pressure and temperature aggravate obviously throughout the whole divergent wall.

Figure 9 presented the pressure and cooling effectiveness contour maps under PR of 3.0, and the film hole position were marked by two dashed lines. It can be seen from fig. 9(a) that there was a bow shaped high pressure zone in front of the film holes exit, the pressure reached a peak value in front of the hole, for the jet obstruction, formed two relative high pressure zones on both sides of the hole with pressure value decreased gradually along the flow direction. The effectiveness contour map was shown in fig. 9(b), which formed corresponding zone distribution caused by pressure. In front of the hole exits, the high pressure zones resulted a lower cooling effectiveness, which broke the accumulation of gas film.

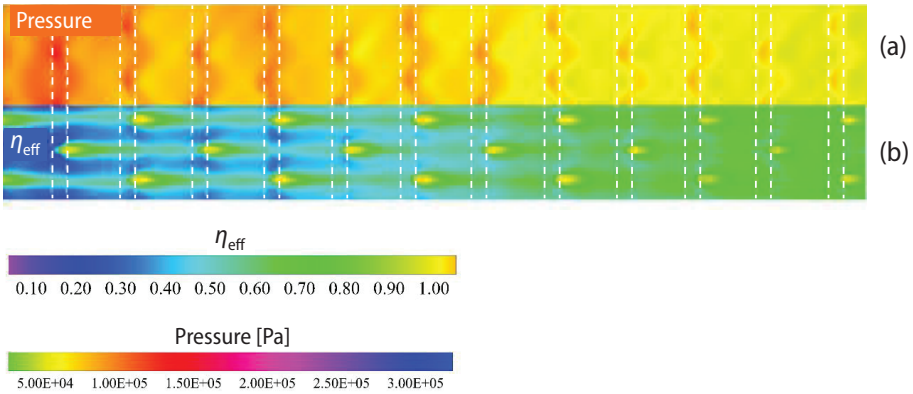

Figure 9. Schematic diagram of the relationship between temperature and pressure under PR = 3

Figure 10 presented parameters distributions at PR of 3.0, and the film hole exits region were marked with shallows. Figures 10(a), and 10(b) presented the cooling effectiveness, temperature, and pressure on line A, while fig. 10(c) showed the pressure and cooling effectiveness contour maps. Figure 10(d) showed the pressure in the longitudinal section passing through holes. By comparison of distributions above, we tried to reveal the relationship among different parameters.

In figs. 10(a), and 10(b), the low cooling effectiveness corresponded to high value of temperature in front of the hole, which was caused by the high stagnation pressure due to jet obstruction. Further, it can be seen from figs. 10(c) and 10(d), the high pressure zone were correspondingly with shock waves position, which were both in front the film exits. It can be concluded the high pressure were induced by the shock wave which caused by the jet obstruction.

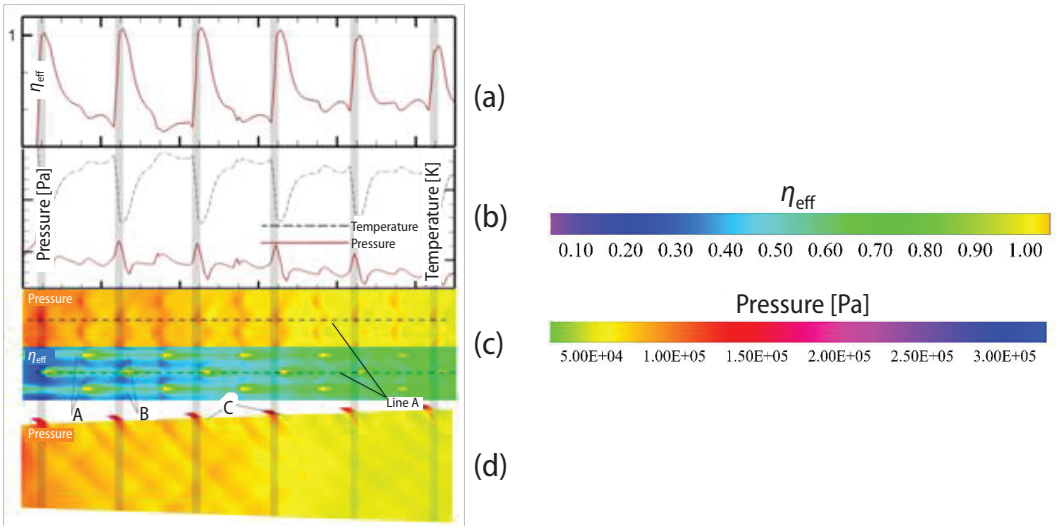

Figure 10. Schematic diagram of parameters in PR 3.0

Effect of the incline angle

To reduce the interference of incline angle with main flow, the effect of inclined angle to cooling effectiveness was investigated through Case 6 and Case 7 under PR 4.

Figures 11 presented the cooling effectiveness on line A under different incline angles. The cooling effectiveness of 15° (Case 7) showed similar fluctuation between holes with that of 30° (Case 6). The decreasing inclined angle led to film adherence enhancement, resulted increasing of cooling effectiveness on walls between holes. However, the decreasing inclined angle also resulted superior heat transfer inside hole, gave a rise of coolant temperature, resulted in a low cooling effectiveness on hole exits region.

Figures 12 presented the pressure on line A under different injection angles. As inclined angle decreased, the pressure of 15° (Case 7) showed similar fluctuation as 30° (Case 6). However, the decrease of angle weakened the interference between the main stream and the coolant jet, reduced the pressure fluctuation between holes, which would deduced the reverse pressure gradient in boundary-layer, and increased the cooling effectiveness. Moreover, the decreasing incline angle also led to a decreasing of the peak value on hole exits region, which mean lower injects velocity, diminished interfere between injects and mainstreams.

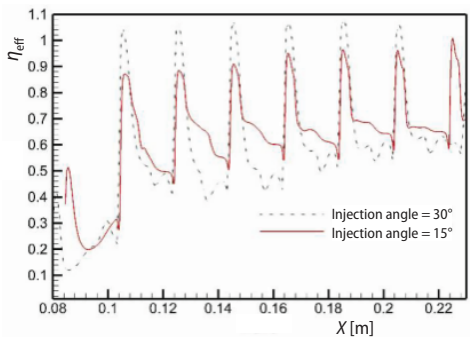

Figure 11. Film cooling effectiveness curves under different film hole incline angles

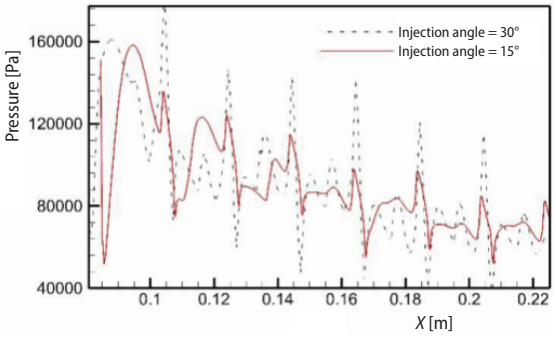

Figure 12. Pressure distributions under different film hole incline angles

Conclusions

In this paper, the numerical investigation of film cooling in supersonic main flow in divergent section had been carried out. It was found that coolant injection led the occurring of shock waves in front of film holes, which exerted extra pressure to boundary-layer, and the interfererance between jets and main flow caused complicated changing of pressure. All the above resulted in corresponding changing of heat transfer. The affection of PR and inclined angle were also studied in the paper.

The main conclusions were as follows.

- In supersonic condition, the block of the coolant jets induced bow oblique shock wave in front of holes. Two oblique bow shaped low pressure zones formed on both sides of the hole, and low pressure induced low cooling effectiveness zones accordingly.
- The shock wave induced reverse pressure gradient in boundary-layer, prevented the film development downstream the hole, led to a decrease and vibration of cooling effectiveness between adjacent holes in line.
- The high stagnation pressure in front rear of hole induced inefficient cooling characteristics at the leading edge of the hole, which destroyed the film developing between holes, decreased the cooling effectiveness accumulation in the rear part.
- The decrease of hole incline angle caused an increase of cooling effectiveness, by reducing reverse velocity gradient caused by shock wave in the boundary-layer and improving film attachment.

References

[1] Bertin, J. J., *Hypersonic Aerothermodynamics*, American Institute of Aeronautics and Astronautics, Inc, New York, USA, 1994
[2] Saunders, O. A., Calder, P. H., Heat Transfer in a Nozzle at Supersonic Speeds, Proceedings of the Institution of Mechanical Engineers, *Part B: Management and engineering manufacture, 1* (1953), 12, pp. 232-239
[3] Adamson, Jr. T. C., On the Structure of Jets from Highly under Expanded Nozzles into Still Air, *Journal of the Aerospace Sciences, 26* (1959), 1, pp. 16-24
[4] Carlson, D. J., Lewis, C. H., Normal Shock Location in under Eexpanded Ggas and Gas-Particle Jets, *AIAA Journal, 2* (1964), 4, pp.776-777
[5] Holden, Michael, S., Experimental Studies of Shock Wave-Boundary Layer Interaction, in: *Laminar and Turbulent Separation Including 3-Dimensional Effects,* Von Karman Institute for Fluid Dynamic, Sint-Genesius-Rode, Belgium,, p. 90
[6] Sandham, N. D., *et al.*, Transitional Shock-Wave/Boundary-Layer Interactions in Hypersonic Flow, *Journal of Fluid Mechanics, 752* (2014), Aug., pp. 349-382
[7] Shimshi, E., *et al.*, Viscous Simulation of Shock-Reflection Hysteresis in over Expanded Planar Nozzles, *Journal of Fluid Mechanics, 635* (2009), Sept., pp. 189-206
[8] Holden, M., *et al.,* Experimental Studies of Shock Wave/Wall Jet Interaction in Hypersonic Flow, *Proceedings*, 28th Aerospace Sciences Meeting, Brisbane, Australia, 1994, 607
[9] Zaman, K., *et al.*, Shock-Induced Boundary-Layer Separation in Round Convergent-Divergent Nozzles, *AIAA Journal, 54* (2015), 2, pp. 434-442
[10] Johnson, A. D., Papamoschou, D., Instability of Shock-Induced Nozzle Flow Separation, *Physics of Fluids, 22* (2010), 1, 016102
[11] Kanda, T., Ono, F., Experimental Studies of Supersonic Film Cooling with Shock Wave Interaction (II), *Journal of Thermophysics and Heat Transfer, 11* (1997), 4, pp. 590-592
[12] Ligrani, P. M., *et al.*, Shock Wave-Film Cooling Interactions in Transonic Flows, *Proceedings*, ASME Turbo Expo 2001: Power for Land, Sea, and Air. American Society of Mechanical Engineers, New Orleans, La., USA, 2001
[13] Juhany, K. A., *et al.,* Influence of Injectant Mach Number and Temperature on Supersonic Film Cooling, *Journal of Thermophysics and Heat Transfer, 8* (1994), 1, pp. 59-67

[14] O'Connor, J. P., Haji-Sheikh, A., Numerical Study of Film Cooling in Supersonic Flow, *AIAA Journal, 30* (1992), 10, pp. 2426-2433
[15] Takita, K., Masuya, G., Effects of Combustion and Shock Impingement on Supersonic Film Cooling by Hydrogen, *AIAA Journal, 38* (2000), 10, pp. 1899-1906
[16] Back, L. H., *et al.,* Comparison of Measured and Predicted Flows through Conical Supersonic Nozzles, with Emphasis on the Transonic Region, *AIAA Journal, 3* (1965), 9, pp. 1606-1614
[17] Aupoix, B., *et al.*, Experimental and Numerical Study of Supersonic Film Cooling, *AIAA Journal, 36* (1998), 6, pp. 915-923
[18] Olsen, G., *et al.*, Experimental Results for Film Cooling in 2-D Supersonic Flow Including Coolant Delivery Pressure, Geometry, and Incident Shock Effects, *Proceedings*, 28th Aerospace Sciences Meeting, Reno, Nev., USA, 1990
[19] Dutton, J. C., Swirling Supersonic Nozzle Flow, *Journal of Propulsion and Power, 3* (1987), 4, pp. 342-349
[20] Peng, W., *et al.*, Effect of Continuous or Discrete Shock Wave Generators on Supersonic Film Cooling, *International Journal of Heat and Mass Transfer, 108* (2017), Part A, pp. 770-783

Paper submitted: April 1, 2019
Paper revised: July 19, 2019
Paper accepted: July 22, 2019